International Journal of Pharmaceutical research and Applications
Volume 11, Issue 5, Sep.-Oct.2026, pp:237-257 www.ijprajournal.com ISSN:2456-4494

Design, characterization and Pharmacological assessment of Zinc oxide based nanoformulations present in Tridax Procumbens and Acalypha Indica using diabetic foot ulcer animal models

Iswariya R[1], Senthil Kumar C[2], Benito Johnson[3], Neelaveni Thangavel[4]
[1]M.Pharm student, Dept of Pharmacology, RVS College of Pharmaceutical Sciences, Sulur, Coimbatore,
[2]Professor, Dept of Pharmacology, RVS College of Pharmaceutical Sciences, Sulur, Coimbatore,
[3]Professor&HOD, Dept of Pharmacology, RVS College of Pharmaceutical Sciences, Sulur, Coimbatore,
[4]Principal, RVS College of Pharmaceutical Sciences, Sulur , Coimbatore.
Corresponding Author: Iswariya R

Date of Submission: 08-09-2026 Date of Acceptance: 17-09-2026

ABSTRACT
Diabetic foot ulcer (DFU) is a major complication of diabetes mellitus associated with delayed wound healing, persistent inflammation, oxidative stress, impaired angiogenesis, and abnormal extracellular matrix remodeling. The present study aimed to design, characterize, and evaluate a green-synthesized zinc oxide (ZnO) nanoformulation containing combined extracts of *Acalypha indica* (AI) and *Tridax procumbens* (TP) for diabetic wound management. Leaves of AI and TP were collected, authenticated, shade-dried, powdered, and extracted using ethanol by Soxhlet extraction. The combined extracts were used for green synthesis of ZnO nanoparticles and characterized by UV-visible spectroscopy, FTIR, particle-size analysis, FE-SEM, and EDX. Molecular docking, drug-likeness, and ADMET studies were performed to investigate the potential interactions of selected phytoconstituents with diabetic wound-healing targets. The nanoformulation was incorporated into a topical hydrogel and evaluated for physicochemical properties. In-vitro wound-healing potential was assessed using a scratch assay, while dermal safety was evaluated through an acute skin irritation study. Streptozotocin-induced diabetic rats were used to assess in-vivo wound-healing activity. Phytochemical screening revealed flavonoids, alkaloids, tannins, and glycosides. Characterization supported ZnO nanoformulation formation, with particle sizes ranging from 183.6–700 nm. The hydrogel exhibited acceptable smoothness, homogeneity, pH, viscosity, and spreadability. No significant dermal irritation or toxicity was observed. The ZnO hydrogel demonstrated the highest wound contraction, reaching 100% on day 14, compared with 68.57% in diabetic control, 80.81% in standard, and 92.12% in combined-extract hydrogel groups. One-way ANOVA showed a significant treatment effect ($p = 0.000085$; $p < 0.05$). Overall, the formulation demonstrated promising topical wound-healing activity and may represent a potential plant-based nanoformulation for DFU management.

Keywords: Diabetic foot ulcer, *Acalypha Indica, Tridax Procumbens,* Zinc oxide nanoparticles, Green synthesis, Nanoformulation, Hydrogel, Wound healing, Molecular docking, Phytochemicals, Diabetes mellitus.

I. INTRODUCTION

DIABETIC FOOT ULCER

Diabetic foot ulcer as defined by the World Health Organization is, "The foot of a diabetic patient that has the potential risk of pathologic consequences, including infection, ulceration, and/or destruction of deep tissues associated with neurologic abnormalities, various degrees of peripheral vascular disease, and/or metabolic complications of diabetes in the lower limb".

EPIDEMIOLOGY

The incidence of diabetic foot has increased due to the worldwide prevalence of diabetes mellitus and the prolonged life expectancy of diabetic patients. These chronic wounds impact patient quality of life and substantially increase the risk of mortality for those affected. DM increases the risk of infection and delays wound healing due to impairment of metabolic activity. On the basis of 2015 prevalence data from the International Diabetes Federation, in Worldwide, 9.1 to 26.1 million people with DM develop DFU annually. Individuals with DM stand a chance of risk for DFU.

The prevalence of DFU in relation to type of DM was 6.5% and 0% for DM type-II and DM type-I

International Journal of Pharmaceutical research and Applications
Volume 11, Issue 5, Sep.-Oct.2026, pp:237-257 www.ijprajournal.com ISSN:2456-4494

respectively. Patients in the age group 51-60 years had the highest frequency of DFU (28.6%), but there was no DFU in those 10-20 years and > 80 years. In the same study 67.2% of patients were males while 32.8% were females.

Pathophysiology of Diabetic Foot Ulcer with Biomarkers

Diabetic foot ulcer (DFU) is a chronic, non-healing wound that develops as a consequence of **persistent hyper glycemia, peripheral arterial disease, peripheral neuropathy, immune dysfunction, and infection**. These factors interact to produce prolonged inflammation, impaired extracellular matrix (ECM) remodeling, poor angiogenesis, and delayed wound closure.

Chronic inflammation and TNF-α

In DFU, the inflammatory response fails to resolve properly. **Tumor necrosis factor-alpha (TNF-α)** is an important pro-inflammatory cytokine that remains elevated in chronic wounds. Increased TNF-α promotes inflammatory signaling, including activation of the **NF-κB pathway**, and contributes to persistent inflammation and tissue injury.

Biomarker: TNF-α ↑

- Pro-inflammatory cytokine
- Promotes chronic inflammation
- Associated with impaired wound healing

MMP-9 and extracellular matrix degradation

Matrix metalloproteinase-9 (MMP-9) is frequently increased in chronic diabetic wounds. Excessive MMP-9 activity causes degradation of important ECM components, including collagen and fibronectin, as well as growth factors required for tissue repair. This results in poor granulation tissue formation and delayed wound closure.

Biomarker: MMP-9 ↑

- Promotes ECM degradation
- Interferes with growth-factor activity
- Contributes to impaired tissue remodeling

TIMPs and MMP/TIMP imbalance

Tissue inhibitors of metalloproteinases (TIMPs), particularly TIMP-1 and TIMP-2, normally regulate MMP activity. In DFU, the balance between MMPs and TIMPs is disrupted. Excessive MMP activity relative to TIMP inhibition promotes continuous ECM degradation.

Biomarker: TIMPs ↓ / MMP:TIMP imbalance ↑

- Reduced control of MMP activity
- Excessive ECM degradation
- Delayed wound repair

VEGF and impaired angiogenesis

Vascular endothelial growth factor (VEGF) is essential for angiogenesis and formation of new blood vessels. Although hypoxia can stimulate VEGF expression, chronic diabetes can result in **abnormal or ineffective VEGF signaling**, producing dysfunctional and leaky vessels rather than adequate functional vascularization. Consequently, oxygen and nutrient delivery to the wound remain inadequate.

Biomarker: VEGF dysregulated

- Regulates endothelial cell proliferation and angiogenesis
- Abnormal signaling contributes to defective vascularization
- Impaired angiogenesis delays wound healing

Overall mechanism

Key Biomarkers in DFU

Biomarker	Change in DFU	Major role	Effect on wound healing
TNF-α	↑	Pro-inflammatory cytokine	Sustains chronic inflammation
MMP-9	↑	ECM-degrading enzyme	Promotes collagen/ECM degradation
TIMP-1/TIMP-2	↓/imbalanced	Inhibit MMPs	Loss of control over ECM degradation
VEGF	Dysregulated	Angiogenesis	Abnormal vascularization and impaired healing

International Journal of Pharmaceutical research and Applications
Volume 11, Issue 5, Sep.-Oct.2026, pp:237-257 www.ijprajournal.com ISSN:2456-4494

Biomarker	Change in DFU	Major role	Effect on wound healing
MMP-9/TIMP ratio	↑	Indicates proteolytic imbalance	Persistent ECM breakdown

Table:1 Biomarker

II. Materials and Methods

Plant Material and Extraction:

Fresh leaves of *Acalypha indica* and *Tridax procumbens* were collected, authenticated, shade-dried and powdered. The powdered materials were separately extracted using ethanol by Soxhlet extraction. They were authenticated by Botanical Survey of India, Southern Regional Center, T.N.A.U Campus, Coimbatore with the authentication no. of *Acalypha indica* BSI/SRC/5/23/2026-27/Tech/1247 & *Tridax procumbens* BSI/SRC/5/23/2026-27/Tech/1246. The collected leaves were thoroughly washed with distilled water to remove dirt and dust. The fresh and clean leaves were air dried in shade at room temperature for 2 to 3 weeks.

- **SHADE DRYING**

  To facilitate preservation of contents, size reduction purposes and preventing the other physiochemical reactions occur due to presence of water. The collected plants and shade dried for 2-3 days.
- **PREPARATION OF COMBINED PLANT EXTRACTS**

EXTRACTION OF TRIDAX PROCUMBENS AND ACALYPHA INDICA

- The fresh leaves of *Tridax Procumbens* and *Acalypha Indica* was collected and dried under the shade and powdered.
- The powdered sample was extracted with ethanol in the method of continuous hot process of extraction in Soxhlet apparatus.

Green Synthesis and Characterization of ZnO Nanoparticles:

The combined plant extract was used for green synthesis of ZnO nanoparticles using a zinc precursor under controlled heating and magnetic stirring. The synthesized nanoparticles were heat-treated and collected. Characterization was performed using UV–Visible spectroscopy, FTIR, zeta potential, FE-SEM and EDX.

In Silico Studies:

Molecular docking was performed against wound-healing-related targets, including TNF-α, MMP-9, TIMP and VEGF, using PyRx/AutoDock. Protein–ligand interactions were analysed using BIOVIA Discovery Studio. ADMET properties were predicted using pkCSM.

Hydrogel Preparation:

Sodium alginate (0.50 g) and ZnO nanoformulation (0.30 g) were dispersed to prepare the formulation. Calcium chloride (2 g) was used as a cross-linking agent. The formulation was added dropwise into calcium chloride solution to form hydrogel beads, which were dried and stored for further evaluation.

In Vitro and In Vivo Studies:

The formulation was evaluated using an L929 fibroblast scratch assay for cell migration and wound-healing activity. In vivo wound-healing activity was assessed using a streptozotocin-induced diabetic excision wound model in rats. Wound contraction was measured at predetermined intervals.

Statistical Analysis:

Results were expressed as mean ± SEM and analysed using one-way ANOVA. A value of $p < 0.05$ was considered statistically significant.

Research Gap

Diabetic foot ulcers are chronic wounds characterized by impaired wound contraction, delayed re-epithelialization, inflammation, oxidative stress and poor collagen formation. Although several conventional wound-healing approaches are available, their effectiveness may be limited by the complex pathological nature of diabetic wounds. Therefore, there is a need to develop safe, effective and affordable plant-based topical formulations for diabetic wound management.

Previous studies have reported the **wound-healing, antioxidant, anti-inflammatory and antimicrobial activities of *Acalypha indica* and *Tridax procumbens* individually**. However, comparatively limited research has investigated the **combined**

International Journal of Pharmaceutical research and Applications
Volume 11, Issue 5, Sep.-Oct.2026, pp:237-257 www.ijprajournal.com ISSN:2456-4494

therapeutic potential of these two medicinal plants specifically in diabetic wound healing. Your thesis literature review also identifies individual pharmacological evidence for both plants.

Furthermore, although plant-mediated synthesis of nanoparticles has attracted considerable interest, there remains a need for further investigation of **plant-based zinc oxide nanoformulations incorporating the combined extracts of *Acalypha indica* and *Tridax procumbens***. The literature reviewed in your thesis supports the use of green synthesis and nanoparticle characterization, but mechanistic evidence for this particular combination remains limited.

Another important gap is the development of a suitable **topical hydrogel delivery system** for the combined plant nanoformulation. Hydrogels can provide convenient topical application and may improve the local delivery of active constituents. Your formulation uses sodium alginate and calcium chloride to produce ionically cross-linked hydrogel granules. However, more systematic investigation is required to establish the relationship between **nanoformulation characteristics, hydrogel properties and wound-healing efficacy**.

LIMITATION OF CURRENT THERAPHY

a. ineffective infection control,
b. failure to address ischemia,
c. high costs,
d. poor patient compliance,
e. resulting in high rates of amputation,
f. Slow wound healing.

METHODOLOGY

1. In-silico molecular docking studies

1.1 Selection of phytoconstituents

The major phytoconstituents reported from *Acalypha indica* and *Tridax procumbens* were selected for computational investigation. Compounds such as **kaempferol and luteolin** were considered based on their reported occurrence in the selected plants and their potential relevance to inflammation, extracellular-matrix remodeling and angiogenesis.

The structures of the selected phytoconstituents were obtained from **PubChem** in suitable three-dimensional formats. The use of experimentally curated protein structures from the Protein Data Bank and computational docking is an established approach in structure-based drug discovery.

1.2 Selection and preparation of target proteins

The diabetic wound-healing-associated targets were selected according to the pathological mechanisms of DFU. The targets used in your thesis were:

- **TNF-α** – inflammatory mediator
- **MMP-9** – extracellular-matrix degradation
- **TIMPs** – regulation of MMP activity
- **VEGF** – angiogenesis

The three-dimensional structures of the selected proteins were retrieved from the **RCSB Protein Data Bank**. Protein preparation involved removal of unnecessary water molecules/heteroatoms, addition of hydrogen atoms and optimization of the receptor structure before docking. The PDB is the established repository for experimentally determined three-dimensional structures of biological macromolecules.

1.3 Ligand preparation

The downloaded ligand structures were converted into suitable three-dimensional docking formats. Hydrogen atoms and appropriate protonation states were assigned, and the ligand structures were energetically optimized before docking.

AutoDock Vina documentation specifically recommends careful ligand preparation, including consideration of protonation state and appropriate molecular structure formats.

1.4 Molecular docking

Molecular docking was performed using **PyRx/AutoDock Vina**. A suitable grid box was defined around the active/binding site of each target protein. The prepared phytoconstituents were docked individually against each target.

AutoDock Vina uses an optimization and scoring procedure to predict ligand binding poses and estimate binding affinity.

The docking results were ranked according to predicted binding energy. **More negative docking scores indicate stronger predicted binding affinity**, although docking scores alone do not establish biological activity.

In your thesis, kaempferol showed predicted binding energies of approximately **−7.0 to −8.5 kcal/mol** against the selected targets, with the strongest reported interaction against TIMPs (−8.5 kcal/mol).

1.5 Protein–ligand interaction analysis

The best-ranked complexes were visualized using **BIOVIA Discovery Studio** or equivalent molecular-visualization software.

The following interactions were examined:

- Hydrogen bonds
- Hydrophobic interactions
- π–π interactions
- Van der Waals interactions
- Interacting amino-acid residues

International Journal of Pharmaceutical research and Applications
Volume 11, Issue 5, Sep.-Oct.2026, pp:237-257 www.ijprajournal.com ISSN:2456-4494

- Binding-site location

The docking findings were interpreted as **predicted molecular interactions**, rather than experimental confirmation of target inhibition. Your thesis also appropriately states that docking findings require experimental confirmation.

2. ADMET and drug-likeness prediction

The selected phytoconstituents were subjected to **in-silico ADMET prediction using pkCSM**.

The parameters considered included:

- Absorption
- Distribution
- Metabolism
- Excretion
- Toxicity
- Physicochemical properties

pkCSM is a published graph-based computational platform developed for prediction of pharmacokinetic and toxicity properties of small molecules.

The predicted ADMET profile was used for preliminary screening of the phytoconstituents before interpretation of their potential therapeutic relevance.

3. Green synthesis of ZnO nanoparticles

The combined ethanolic extracts of *A. indica* and *T. procumbens* were used for green synthesis of ZnO nanoparticles.

Your thesis uses **zinc sulphate** as the precursor and describes magnetic-stirring-based green synthesis.

Procedure

The combined plant extract was mixed with the zinc precursor solution under controlled stirring and temperature conditions. The reaction mixture was continuously stirred to facilitate interaction between phytochemicals and zinc ions.

A visible change in colour was considered a preliminary indication of nanoparticle formation. Your experimental observations describe gradual development of a dark-green colour following addition of the combined plant extract.

The resulting material was collected, dried and subjected to physicochemical characterization.

Plant-mediated ZnO synthesis is supported by several published studies. For example, green synthesis using *Cayratia pedata* employed plant extract with a zinc precursor followed by drying and characterization by UV–Vis, FTIR, XRD, FE-SEM and EDX.

A particularly relevant recent study reported green ZnO synthesis using *Acalypha indica* leaf extract and characterized the resulting nanoparticles by UV–Vis, FTIR, XRD and SEM.

4. Characterization of ZnO nanoparticles

The synthesized ZnO nanoformulation was characterized using complementary analytical techniques to establish its **optical, chemical, structural, morphological and surface properties**.

Table:2 Characterization of ZnO nanoparticles

Characterization	Purpose
UV–Visible spectroscopy	Confirmation of nanoparticle formation and optical absorption
FTIR	Identification of functional groups and phytochemical capping
XRD	Crystalline structure and crystallite size
FE-SEM	Surface morphology and particle distribution
EDX	Elemental composition
DLS	Hydrodynamic particle size
Zeta potential	Surface charge and colloidal stability

These techniques are widely used in published green-synthesized ZnO nanoparticle studies.

4.1 UV–Visible spectroscopy

A suitable dispersion of the synthesized ZnO nanoparticles was prepared in distilled water and analyzed using a UV–Visible spectrophotometer.

The absorption spectrum was recorded over an appropriate wavelength range, and the characteristic absorption maximum was used as preliminary evidence of ZnO nanoparticle formation.

Published plant-mediated ZnO studies have reported characteristic absorption bands in the UV region; the exact wavelength varies with particle size, morphology and synthesis conditions. For example, *Acalypha indica*-mediated ZnO nanoparticles showed an absorption peak around **384 nm**, whereas other plant-mediated ZnO preparations have shown different maxima.

International Journal of Pharmaceutical research and Applications
Volume 11, Issue 5, Sep.-Oct.2026, pp:237-257 www.ijprajournal.com ISSN:2456-4494

Therefore, the exact UV maximum obtained in your experiment should be reported rather than using a literature value.

4.2 FTIR analysis

FTIR spectroscopy was performed to identify functional groups associated with phytochemicals present in the plant extract and on the surface of the synthesized nanoparticles.

In your experimental procedure, the dried sample was placed directly on an ATR crystal and analyzed from **4000–600 cm^{-1}**, at **4 cm^{-1} resolution with 32 scans**.

The nanoparticle spectrum was compared with the plant-extract spectrum to identify changes or shifts in characteristic peaks. Such changes can provide evidence for the involvement of phytochemical functional groups in nanoparticle formation and surface stabilization.

Published *Acalypha indica* ZnO research identified Zn–O vibrations around **476 and 512 cm^{-1}** together with surface-associated phenolic, aliphatic and carbonyl groups.

4.3 X-ray diffraction analysis

XRD was performed to determine the crystalline structure of the synthesized ZnO nanoparticles.

The dried nanoparticle sample was subjected to XRD analysis using Cu-Kα radiation where applicable. The obtained diffraction peaks were compared with standard ZnO reference patterns.

The crystallite size may be estimated using the Scherrer equation:

D=Kλβcos⁡θD=\frac{K\lambda}{\beta\cos\theta}

where:

- **D** = crystallite size
- **K** = Scherrer constant
- **λ** = X-ray wavelength
- **β** = FWHM of the diffraction peak
- **θ** = Bragg angle

Published plant-mediated ZnO studies commonly report the characteristic **hexagonal wurtzite ZnO structure**.

4.4 FE-SEM analysis

FE-SEM was performed to determine:

- Particle morphology
- Shape
- Surface characteristics
- Particle distribution
- Aggregation

According to your thesis, the dried sample was mounted on an aluminium stub using conductive adhesive, sputter-coated and analyzed under high vacuum. The FE-SEM was operated at approximately **15 kV**, with images recorded at different magnifications.

Published green ZnO research similarly uses SEM/FE-SEM to assess nanoparticle morphology.

4.5 EDX analysis

EDX analysis was performed together with electron microscopy to determine the elemental composition of the synthesized material.

The presence of characteristic signals corresponding to **zinc and oxygen** supports the formation of ZnO nanoparticles.

Plant-mediated ZnO studies have used EDX to confirm zinc and oxygen composition.

4.6 DLS and zeta-potential analysis

Dynamic light scattering was used to determine the **hydrodynamic particle size distribution** of the nanoparticle dispersion.

Zeta potential was measured to evaluate the surface charge and provide an indication of colloidal stability.

Your thesis specifies that the sample was dispersed in double-distilled water, sonicated for **10–15 min**, filtered and measured at approximately **25°C**, with measurements performed in triplicate.

Published ZnO studies similarly employ DLS and zeta potential as complementary measurements of nanoparticle size and colloidal stability.

5. Hydrogel formulation

The prepared ZnO nanoformulation was incorporated into a **sodium-alginate hydrogel system**.

The formulation used in your thesis contains:

- Sodium alginate – **0.50 g**
- ZnO nanoformulation – **0.30 g**
- Calcium chloride – **2.0 g**

The sodium alginate was dispersed in an appropriate aqueous medium with continuous stirring. The ZnO nanoformulation was incorporated to obtain a homogeneous formulation.

The formulation was subsequently subjected to ionic cross-linking using calcium ions. Calcium chloride was used as the cross-linking agent to form the alginate hydrogel.

Your thesis identifies sodium alginate/calcium chloride hydrogel formulation as part of the experimental plan.

6. In-vitro scratch wound-healing assay

- Cell culturing and maintenance

  Serum free Dulbecco's modified eagle medium (DMEM)(SFM)

International Journal of Pharmaceutical research and Applications
Volume 11, Issue 5, Sep.-Oct.2026, pp:237-257 www.ijprajournal.com ISSN:2456-4494

- **Preparation of serum media**

  Fetal bovine serum (FBS) obtained commercially from Himedia was used.

  In 450 ml of DMEM medium (SFM), 50 ml of FBS (10% FBS) was added and were sterile filtered and stored at 2-8°C.

- **Trypsin-ethylene diamine tetra acetic acid (EDTA) solution**

  Ready to use trypsin (0.25%)-EDTA (0.02%) solution purchased from Himedia was used for trypsinization**.**

- **Procurement of cell line and sub-culturing**

  The LN929 lines were maintained in 5% CO2 incubator at 37 °C with DMEM medium (10% FBS and 1% antibiotic/anti-mycotic solution). Once the cells reached confluency, they were further sub-cultured using with trypsin-EDTA solution for 2 minutes, removed, and then resuspended in serum medium after five minutes. The resuspended cells were then used for further sub-culturing and experimental analysis wound Healing.

- **Wound healing**
  - $1X10^4$ L929 cells were seeded in 6 well plates and kept at 37°C in a 5% CO_2 humidified incubator for cells to be attached.
  - After confluency is attained, the existing serum media were removed.
  - The treatment grouping and plan is provided as follows:

    Cells were scratched using 200µl sterile tips, washed twice using PBS. Then sample extract was treated with IC50 Value at 0,24, AND 48 hours to check the efficacy. At the end of all treatment hours, the morphological changes were observed in the "Zoe fluorescent microscope – Biorad" at bright field.

7. In-vivo diabetic wound-healing study

7.1 Ethical approval and animal welfare

The animal experiment should be conducted only after approval from the appropriate institutional animal ethics committee and according to applicable national regulations.

The pharmacology and acute toxicity protocols were approved by Institutional Animal Ethics Committee with IAEC NO. RVSCOPS/IAEC-2026-2027.

The study should report animal species, strain, sex, age/weight, housing, experimental procedures, randomization, outcome measures and statistical methods.

7.2 Experimental animals

Healthy laboratory rats of an appropriate strain were housed under controlled environmental conditions with standard feed and water provided ad libitum.

Animals were acclimatized before commencement of the experiment.

7.3 Induction of diabetes

Diabetes was induced using **streptozotocin (STZ)** according to the approved experimental protocol.

A published diabetic wound model used STZ to induce hyperglycemia and confirmed diabetes using blood-glucose measurements before creating the wound.

Another study specifically investigated *T. procumbens*-derived ZnO nanoparticles using an STZ-induced diabetic rat model, supporting the relevance of this model to the plant/ZnO research area.

For your thesis, the exact STZ dose, route, fasting procedure and glucose cut-off should be written exactly according to the protocol actually used in your laboratory and approved by your ethics committee.

7.4 Creation of excision wound

Following confirmation of diabetes, animals were appropriately anesthetized and the dorsal region was prepared aseptically.

A standardized full-thickness excisional wound was created using an appropriate sterile wound-making technique.

A published ZnO-hydrogel diabetic wound model used standardized full-thickness dorsal wounds in STZ-induced diabetic rats to evaluate topical ZnO hydrogel treatment.

8. Experimental groups

Based on your thesis, the study can be represented as follows:

Group	Treatment
Group I	Normal/negative control

International Journal of Pharmaceutical research and Applications
Volume 11, Issue 5, Sep.-Oct.2026, pp:237-257 www.ijprajournal.com ISSN:2456-4494

Group	Treatment
Group II	Diabetic/positive control
Group III	Standard treatment
Group V – Test	ZnO nanoformulation hydrogel containing combined *A. indica* + *T. procumbens*

Your thesis reports these treatment groups and compares wound contraction over the experimental period.

9. Topical treatment

The respective formulations were applied topically to the wound according to the predefined treatment schedule. The wound area was monitored at predetermined intervals.

The wound was protected from contamination where required using suitable sterile dressing.

Published diabetic wound studies have similarly evaluated topical ZnO-containing hydrogel systems against appropriate control groups.

10. Wound contraction

The wound area was measured at predetermined intervals. Your thesis records measurements on:

Day 0 → Day 4 → Day 9 → Day 14.

The percentage wound contraction was calculated using:

% Wound Contraction=Initial wound area−Remaining wound areaInitial wound area×100\%\,Wound\ Contraction = \frac{Initial\ wound\ area-Remaining\ wound\ area} {Initial\ wound\ area}\times100

A higher percentage of wound contraction indicates greater progression toward wound closure.

Your thesis reported the highest 14-day wound contraction for the ZnO hydrogel test group.

11. Epithelialization period

The **epithelialization period** was recorded as the time required for complete coverage of the wound by newly formed epithelium.

A shorter epithelialization period indicates faster wound repair.

This parameter is particularly relevant because published *Tridax procumbens* wound-healing studies evaluated epithelialization, wound contraction and hydroxyproline content in diabetic and non-diabetic animal models.

12. Hydroxyproline estimation

Hydroxyproline content was estimated in regenerated wound tissue as an indirect indicator of **collagen deposition**.

Increased hydroxyproline content is interpreted as evidence of increased collagen synthesis and extracellular-matrix formation during the proliferative/remodeling phase of wound healing.

Published *T. procumbens* wound-healing research evaluated hydroxyproline along with wound contraction and histopathology and reported increased healing-associated tissue parameters.

14. Histopathological examination

At the predetermined endpoint, wound tissue samples were collected and processed for histopathological examination.

The tissue sections were evaluated for:

- Re-epithelialization
- Granulation tissue formation
- Fibroblast proliferation
- Collagen deposition
- Inflammatory-cell infiltration
- Angiogenesis
- Overall tissue organization

Histopathological evaluation provides morphological evidence supporting the quantitative wound-contraction findings.

15. Biomarker evaluation

To investigate the possible mechanism underlying the wound-healing effect, relevant inflammatory, ECM-remodeling and angiogenic biomarkers may be evaluated.

TNF-α

TNF-α was selected as a marker of persistent inflammation.

Expected therapeutic effect:

TNF−α↓TNF-\alpha \downarrow

MMP-9

MMP-9 was selected as a marker of excessive extracellular-matrix degradation.

Expected therapeutic effect:

MMP−9↓MMP-9 \downarrow

TIMP-1/TIMP-2

TIMPs regulate MMP activity and therefore provide information regarding the **MMP/TIMP balance**.

Expected therapeutic effect:

TIMP regulation↑TIMP\ regulation \uparrow

VEGF

VEGF was selected as a marker associated with angiogenesis and vascular repair.

Expected therapeutic effect:

VEGF normalization↑VEGF\ normalization \uparrow

International Journal of Pharmaceutical research and Applications
Volume 11, Issue 5, Sep.-Oct.2026, pp:237-257 www.ijprajournal.com ISSN:2456-4494

Your thesis identifies TNF-α, MMP-9, TIMPs and VEGF as molecular targets associated with inflammation, ECM remodeling and angiogenesis in diabetic wound healing.

16. Statistical analysis

Experimental data should be expressed as **mean ± SD or mean ± SEM**, as appropriate.

For comparison of multiple experimental groups, **one-way ANOVA** followed by an appropriate post-hoc test may be used

A value of: $p<0.05p<0.05$ may be considered statistically significant.

Results and Discussion

Molecular docking demonstrated favourable interactions of the selected phytoconstituents with wound-healing-associated targets.

Kaempferol showed stronger predicted binding than luteolin, with binding energies of −7.0 kcal/mol for TNF-α, −8.4 kcal/mol for MMP-9, −8.5 kcal/mol for TIMPs and −8.2 kcal/mol for VEGF.

These findings suggest a possible role of these phytoconstituents in regulating inflammation, extracellular-matrix remodelling and angiogenesis; however, docking results require experimental confirmation.

1.MMP-9:5OE4-KAEMPFEROL

2D COMPLEX OF MMP-9 AND LIGANDGS INTERACTIONS

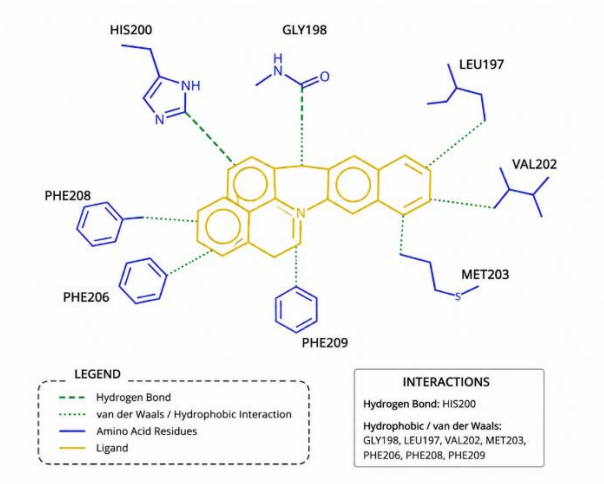

3D COMPLEX OF MMP-9 AND LIGANDGS INTERACTIONS

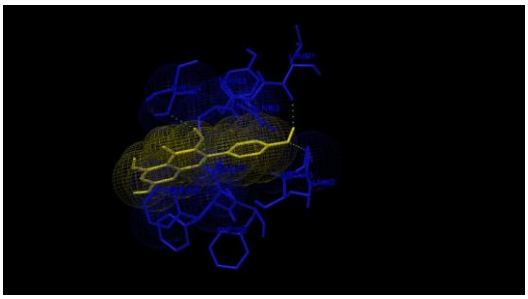

2.MMP-9:5OE4-LUTEOLIN

2D COMPLEX OF MMP-9 AND LIGANDGS INTERACTIONS

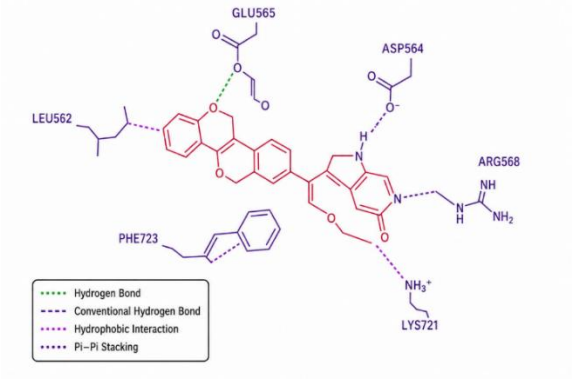

3D COMPLEX OF MMP-9 AND LIGANDGS INTERACTIONS

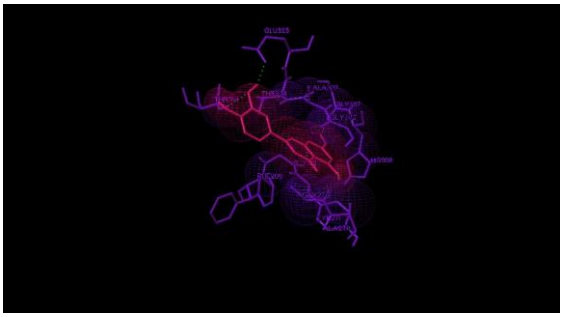

3.TNF-α:4G3Y-KAEMPFEROL

2D COMPLEX OF TNF-α AND LIGANDGS INTERACTIONS

International Journal of Pharmaceutical research and Applications
Volume 11, Issue 5, Sep.-Oct.2026, pp:237-257 www.ijprajournal.com ISSN:2456-4494

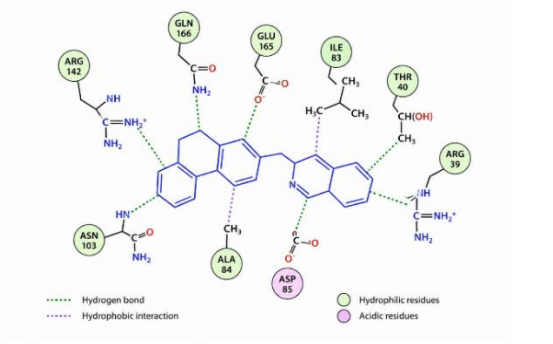

3D COMPLEX OF TNF-α AND LIGANDGS INTERACTIONS

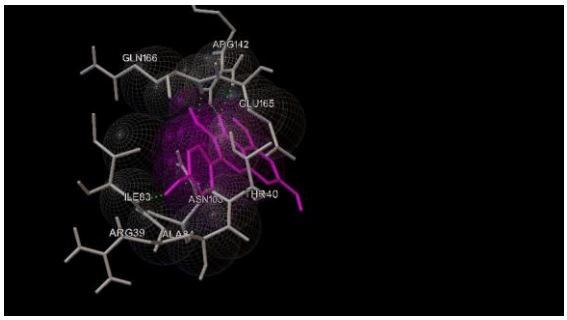

4.TNF-α:4G3Y-LUTEOLIN
2D COMPLEX OF TNF-α AND LIGANDGS INTERACTIONS

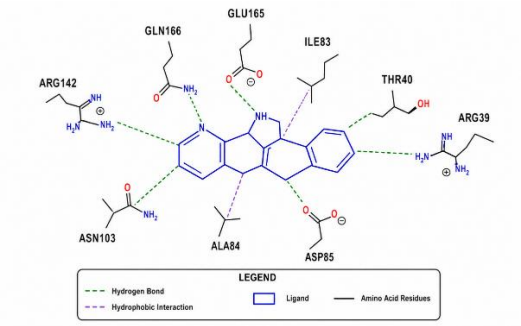

3D COMPLEX OF TNF-α AND LIGANDGS INTERACTIONS

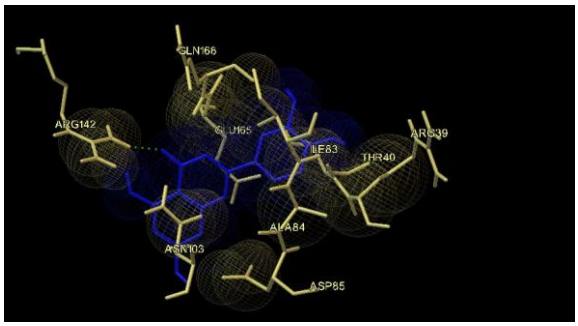

5.TIMPs:6N9D-KAEMPFEROL
2D COMPLEX OF TIMPs AND LIGANDGS INTERACTIONS

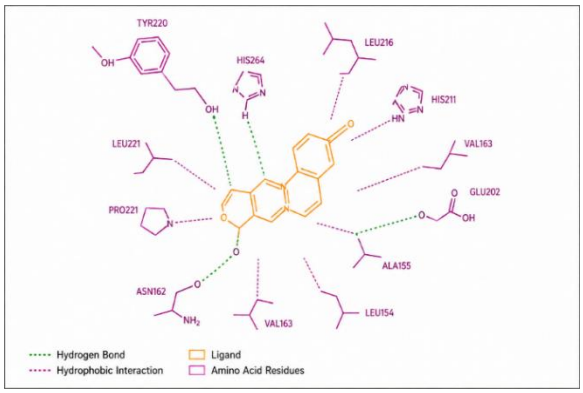

3D COMPLEX OF TIMPs AND LIGANDGS INTERACTIONS

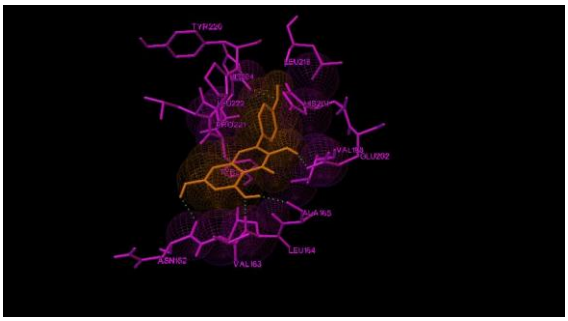

6.TIMPs:6N9D-LUTEOLIN
2D COMPLEX OF TIMP**s** AND LIGANDGS INTERACTIONS

International Journal of Pharmaceutical research and Applications
Volume 11, Issue 5, Sep.-Oct.2026, pp:237-257 www.ijprajournal.com ISSN:2456-4494

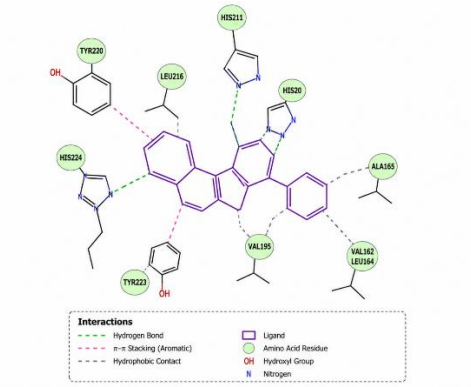

3D COMPLEX OF TIMPs AND LIGANDGS INTERACTIONS

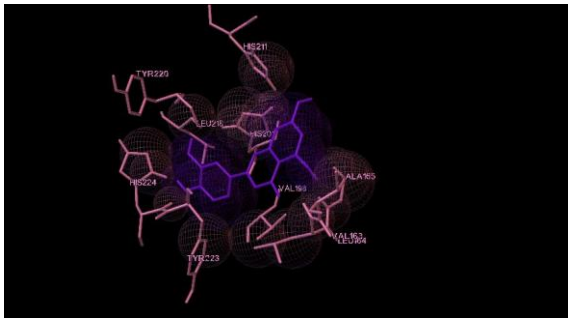

7.VEGF :2VPF-KAEMPFEROL

2D COMPLEX OF VEGF AND LIGANDGS INTERACTIONS

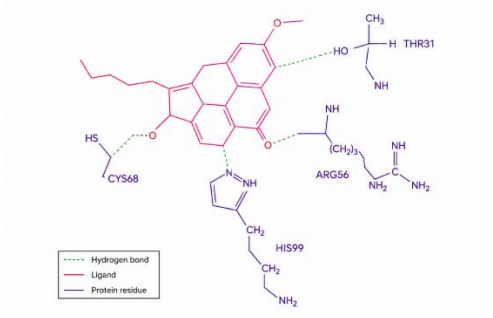

3D COMPLEX OF VEGF AND LIGANDGS INTERACTIONS

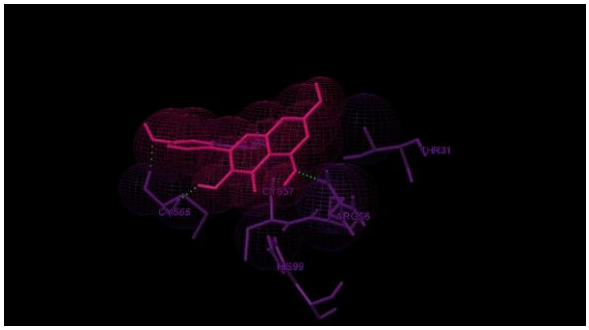

8.VEGF :2VPF-LUTEOLIN

2D COMPLEX OF VEGF AND LIGANDGS INTERACTIONS

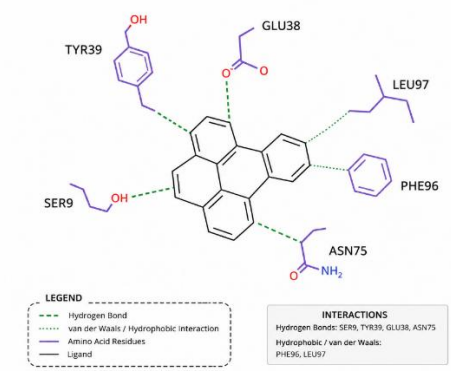

3D COMPLEX OF VEGF AND LIGANDGS INTERACTIONS

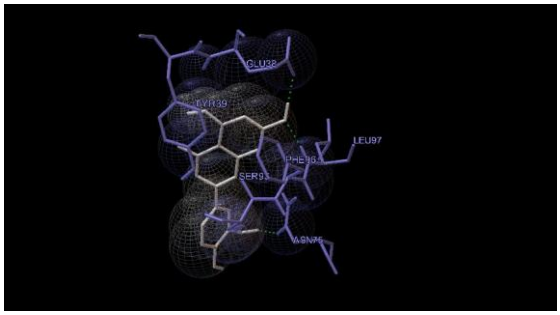

***IN SILICO* BINDING ENERGY AND INTERPRETATION**

Table 3:Binding Energy and Interpretation

S. No.	Target protein	Kaempferol (kcal/mol)	Luteolin (kcal/mol)	Better binding affinity	Interpretation
1	**MMP-9**	**−8.4**	−7.8	**Kaempferol**	Kaempferol showed stronger binding affinity than luteolin,

International Journal of Pharmaceutical research and Applications
Volume 11, Issue 5, Sep.-Oct.2026, pp:237-257 www.ijprajournal.com ISSN:2456-4494

S. No.	Target protein	Kaempferol (kcal/mol)	Luteolin (kcal/mol)	Better binding affinity	Interpretation
					indicating a potentially more stable interaction with MMP-9.
2	**TNF-α**	**−7.0**	−6.6	**Kaempferol**	Kaempferol exhibited better binding than luteolin, suggesting stronger interaction with TNF-α.
3	**TIMPs**	**−8.5**	−7.5	**Kaempferol**	Kaempferol showed the strongest binding affinity among the tested compounds for TIMPs.
4	**VEGF**	**−8.2**	−7.3	**Kaempferol**	Kaempferol demonstrated stronger binding affinity toward VEGF compared with luteolin.

Interpretation

The molecular docking results demonstrated that **both kaempferol and luteolin exhibited favorable binding affinities** toward the selected diabetic foot ulcer-associated targets. Since **more negative binding energy indicates stronger predicted binding affinity**, kaempferol showed superior binding against all four targets.

Among the selected targets, **kaempferol showed the highest binding affinity toward TIMPs (−8.5 kcal/mol)**, followed by **MMP-9 (−8.4 kcal/mol)** and **VEGF (−8.2 kcal/mol)**. Luteolin showed binding energies of **−7.5, −7.8, and −7.3 kcal/mol** toward TIMPs, MMP-9, and VEGF, respectively.

Overall, the docking results suggest that **kaempferol may have a stronger potential interaction with the selected molecular targets associated with inflammation, extracellular-matrix remodeling, and angiogenesis in diabetic wound healing**. However, docking scores alone do not establish biological activity and should be supported by experimental studies.

"Molecular docking analysis revealed that kaempferol exhibited better binding affinity than luteolin against all the selected targets. The highest binding affinity was observed for kaempferol against TIMPs (−8.5 kcal/mol), followed by MMP-9 (−8.4 kcal/mol), VEGF (−8.2 kcal/mol), and TNF-α (−7.0 kcal/mol).

These findings suggest that kaempferol may possess favorable molecular interactions with key targets involved in inflammation, extracellular matrix degradation, and angiogenesis during diabetic foot ulcer healing."

The combined ethanolic extracts of *Acalypha indica* and *Tridax procumbens* produced a greenish semisolid extract with a percentage yield of 24.71%.

Green synthesis of the ZnO nanoformulation resulted in a gradual colour change to dark green, indicating nanoparticle formation.

ZnO Nanoformulations

UV–Visible analysis

UV–Visible analysis showed characteristic absorption bands at 220, 270–292, 400 and 660 nm, with maximum absorbance at 220 nm (1.987) and a prominent absorption at 400 nm (1.254).

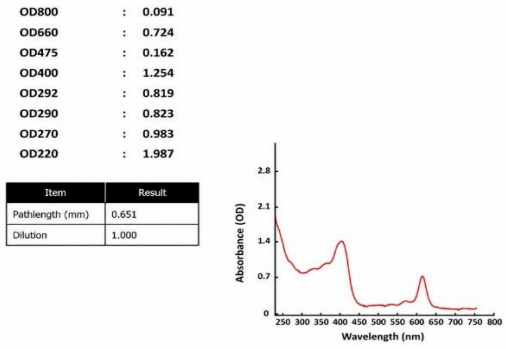

Fig 1:Time dependent UV-Vis absorbance spectra by UV for ZnO nanoformulation synthesis

International Journal of Pharmaceutical research and Applications
Volume 11, Issue 5, Sep.-Oct.2026, pp:237-257 www.ijprajournal.com ISSN:2456-4494

FTIR analysis

FTIR analysis further indicated the involvement of phytochemical functional groups in nanoparticle formation and surface functionalization.

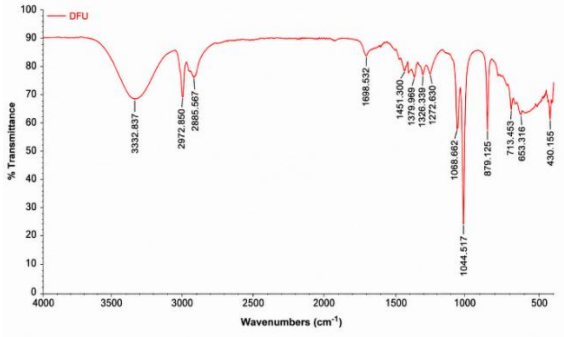

Fig 2:FTIR spectrum of combined extract and ZnO NPs

Zeta potential

The zeta potential of the prepared DFU nanoformulation was found to be −50.5 mV at 25 °C. The high negative zeta potential indicates sufficient surface charge and strong electrostatic repulsion between the nanoparticles, suggesting good colloidal stability with reduced aggregation tendency. The sharp distribution peak observed around −50.5 mV further supports the uniformity and stability of the prepared nanoformulation.

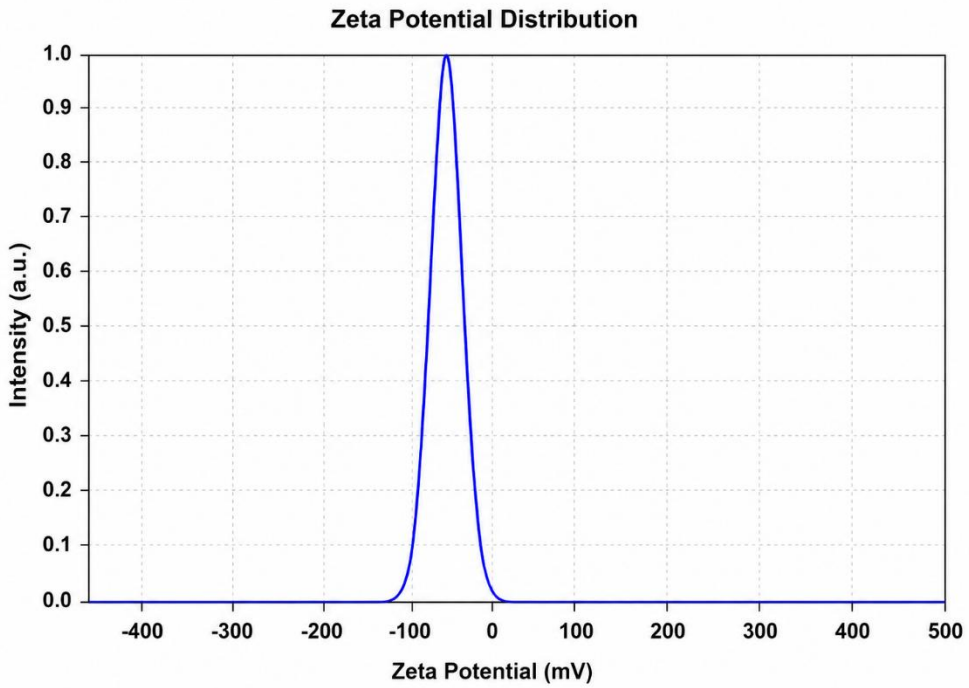

Fig 3: Particle size distribution of synthesized ZnO by DLS based on intensity

FE SEM:

Field emission scanning electron microscopy was performed to evaluate the surface morphology of the green-synthesized ZnO nanoformulation prepared using Acalypha indica and Tridax procumbens extracts. The FESEM micrograph demonstrated the formation of irregularly shaped and aggregated nanostructured domains with a compact and interconnected morphology. Selected nanoscale features exhibited dimensions of 124.34 nm, 92.61 nm, and 87.37 nm, corresponding to an approximate mean characteristic size of 101.44 nm. The observed aggregation may be attributed to the high surface energy of ZnO nanostructures and interparticle interactions occurring during synthesis and drying. The variation in size and morphology may also reflect the influence of plant-derived phytoconstituents involved in the reduction, stabilization, and growth of the ZnO nanostructures. Overall, the FESEM observations support the successful formation of ZnO nanostructured material through a green synthesis approach, although quantitative particle-size distribution analysis using multiple images and a larger number of particles is recommended for definitive size characterization.

International Journal of Pharmaceutical research and Applications
Volume 11, Issue 5, Sep.-Oct.2026, pp:237-257 www.ijprajournal.com ISSN:2456-4494

The FESEM analysis of the green-synthesized ZnO nanoformulation prepared using the combined extracts of Acalypha indica and Tridax procumbens revealed an irregular and heterogeneous surface morphology. The micrograph demonstrated the presence of densely packed, interconnected, and agglomerated ZnO structures with rough surface characteristics. Flake-like and plate-like morphological features were observed along with irregular cavities and porous regions distributed throughout the particle matrix.

The observed particles were not uniformly dispersed as isolated individual nanoparticles; instead, they appeared to form larger aggregates. This aggregation may be attributed to strong interparticle interactions and the high surface energy of ZnO nanoparticles. The porous and rough morphology may provide an increased effective surface area and a greater number of exposed surface-active sites.

Overall, the FESEM image confirms the successful formation of a nanostructured ZnO-based material with an aggregated and heterogeneous morphology. However, accurate determination of individual nanoparticle size requires higher-resolution imaging.

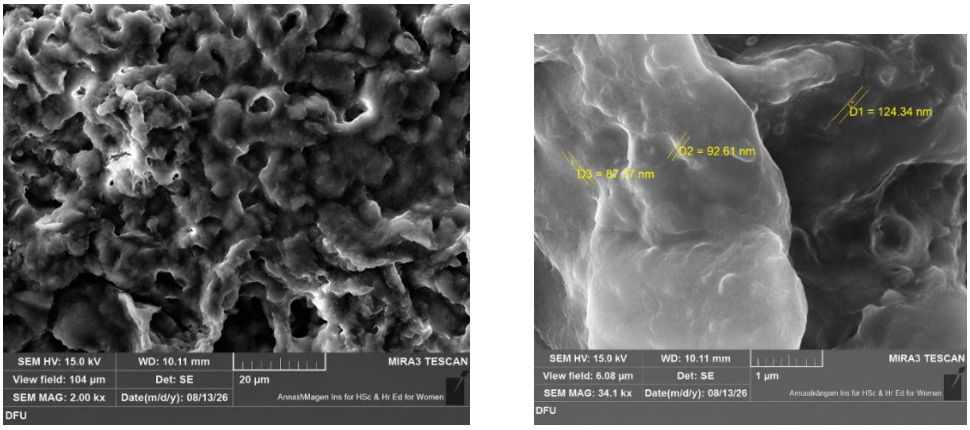

FE SEM

ENERGY DISPERSIVE SPECTROSCOPY

The EDAX analysis revealed that the sample mainly consists of Zinc (C) and Oxygen (O). The quantitative results showed that Zinc is the major element with a weight percentage of 68.65% and an atomic percentage of 75.25%, while Oxygen is present with a weight percentage of 28.14% and an atomic percentage of 23.16%. The EDAX spectrum displayed clear and well defined peaks corresponding to these elements, confirming their presence in the selected area of the sample. The higher concentration of Zinc indicates that the sample is predominantly carbon-based, while the presence of Oxygen may be due to surface oxidation or oxygen containing functional groups. The absence of other elemental peaks suggests that the sample is relatively pure and free from significant impurities. Thus, EDAX proved to be an effective technique for identifying and quantifying the elemental composition of the sample. Overall, the EDAX results support the elemental composition of the analyzed formulation/sample

International Journal of Pharmaceutical research and Applications
Volume 11, Issue 5, Sep.-Oct.2026, pp:237-257 www.ijprajournal.com ISSN:2456-4494

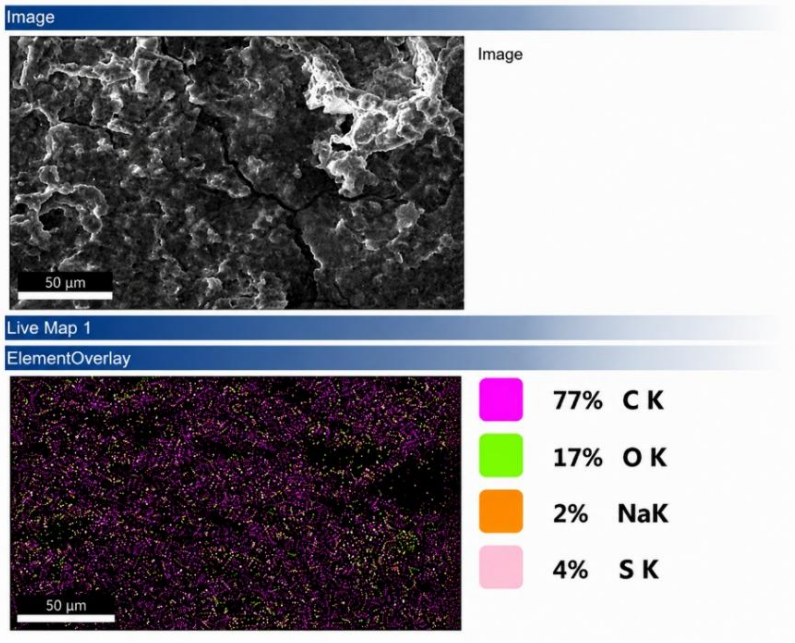

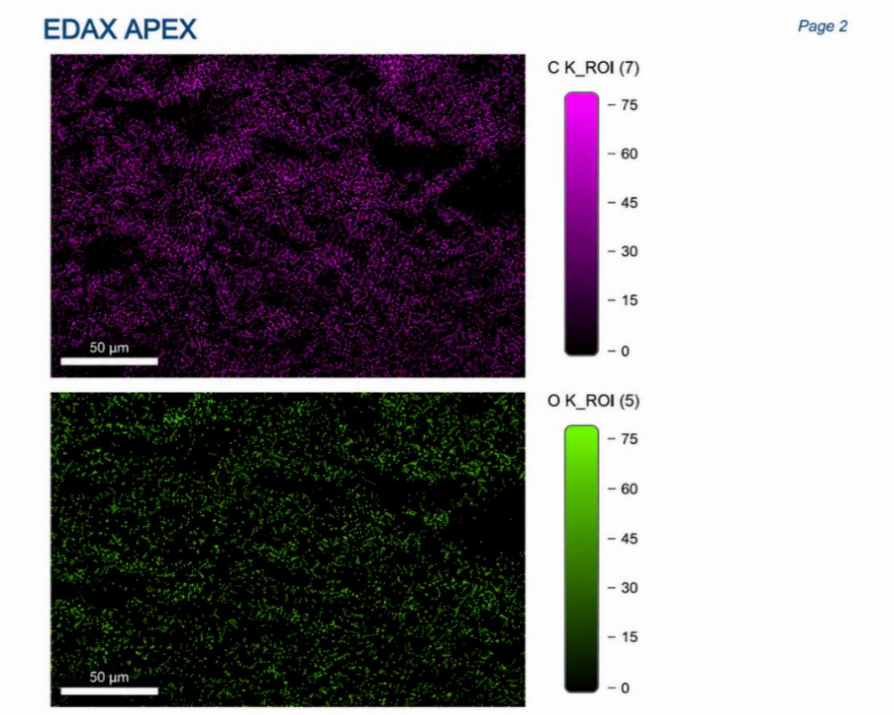

International Journal of Pharmaceutical research and Applications
Volume 11, Issue 5, Sep.-Oct.2026, pp:237-257 www.ijprajournal.com ISSN:2456-4494

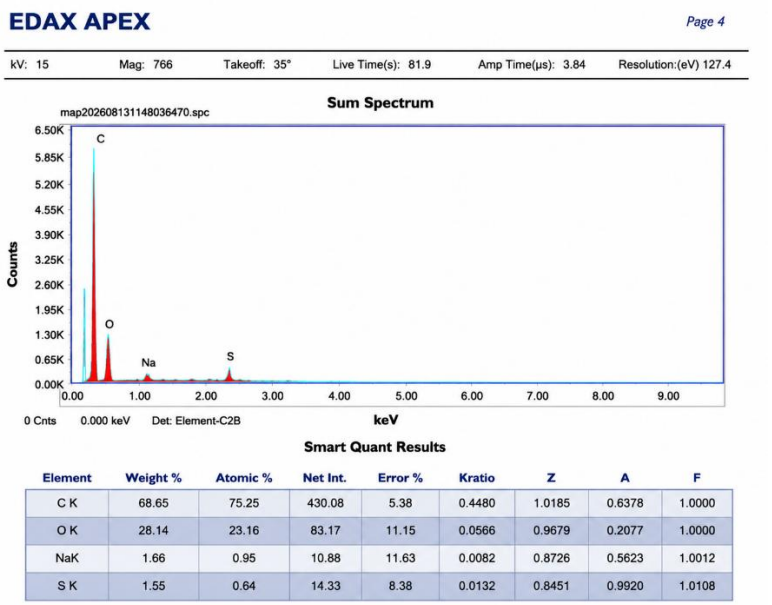

Element	Weight %	Atomic %	Net Int.	Error %	Kratio	Z	A	F
C K	68.65	75.25	430.08	5.38	0.4480	1.0185	0.6378	1.0000
O K	28.14	23.16	83.17	11.15	0.0566	0.9679	0.2077	1.0000
NaK	1.66	0.95	10.88	11.63	0.0082	0.8726	0.5623	1.0012
S K	1.55	0.64	14.33	8.38	0.0132	0.8451	0.9920	1.0108

- **EVALUATION OF HYDROGEL**
  - **SWELLING INDEX**

Swelling Index = 141.67%

This means that, on average, the dry granules exhibited an approximately **141.67% increase in weight after swelling** under the specified experimental conditions.

1. **Results**

Table 4:Swelling index values

S. No.	Initial dry weight (W_0) (mg)	Swollen weight (W_t) (mg)	Swelling Index (%)
1	100	171	71
2	100	249	149
3	100	305	205
Mean	—	—	**141.67**

The swelling index of the prepared hydrogel granules was determined in triplicate. The swelling index values for the three samples were 71%, 149%, and 205%, respectively. The mean swelling index was found to be 141.67%. The results indicate that the prepared hydrogel granules possess appreciable liquid absorption and swelling capacity.

***IN VITRO*- SCRATCH ASSAY**

International Journal of Pharmaceutical research and Applications
Volume 11, Issue 5, Sep.-Oct.2026, pp:237-257 www.ijprajournal.com ISSN:2456-4494

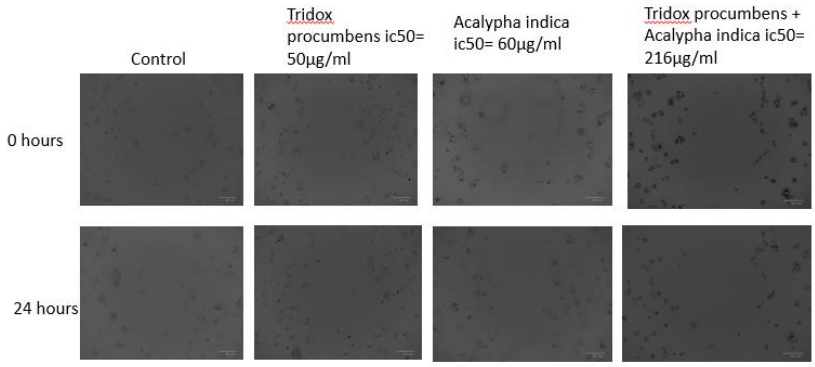

Results:

The wound-healing assay demonstrated a treatment-dependent reduction in cellular migration. Control cells showed greater spreading and migration into the scratched area, resulting in progressive wound closure. In contrast, treated cells exhibited reduced migration, increased cellular rounding and detachment, and incomplete closure of the wound area. The inhibitory effect appeared more pronounced at higher treatment conditions."

***IN-VIVO* DIABETIC WOUND HEALING ACTIVITY**

The in-vivo study demonstrated progressive wound contraction in all groups, with the diabetic control showing delayed healing. On day 14, wound contraction was 68.57% in the diabetic control, 92.12% in the standard group, 80.81% in the combined-extract hydrogel group and 100% in the ZnO hydrogel group. The ZnO hydrogel therefore produced the highest wound contraction and complete wound closure by day 14.

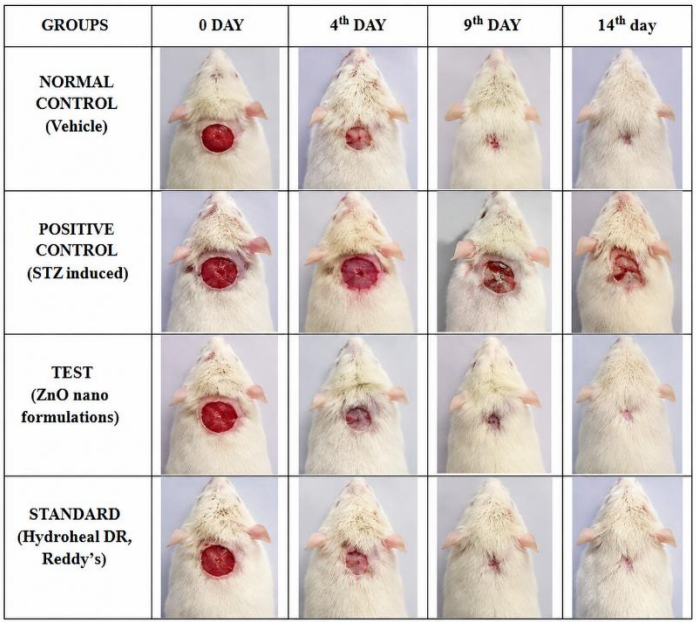

Wound healing observation in rats

On comparing positive control with test , the p-value obtained is 0.007963, which is less than 0.05. Hence the result is statistically significant. Since the p-value for the treatment effect is 0.000085 which is less than 0.05, we can conclude that the treatment effect is statistically significant.

International Journal of Pharmaceutical research and Applications
Volume 11, Issue 5, Sep.-Oct.2026, pp:237-257 www.ijprajournal.com ISSN:2456-4494

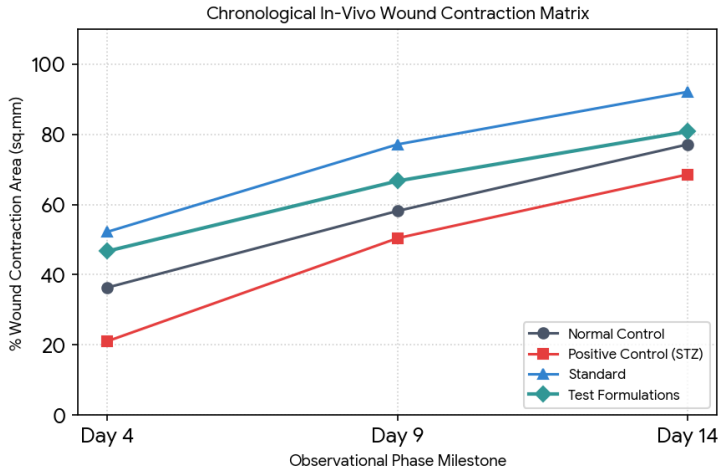

Overall, the findings indicate that the combined *A. indica–T. procumbens* ZnO hydrogel exhibited promising wound-healing activity in the diabetic wound model and performed better than the combined-extract hydrogel alone. The study provides preliminary experimental and computational support for further investigation of this plant-based nanoformulation for diabetic wound management.

References

[1]. Ministry of Health & Family Welfare, Government of India. The Diabetic foot Prevention and management in India [Internet]. 2016. Available from: http://clinicalestablishments.gov.in/WriteReadData/5381.pdf.

[2]. Armstrong, D. G., Boulton, A. J. M., & Bus, S. A. (2017). Diabetic foot ulcers and their recurrence. *The New England Journal of Medicine*, *376*(24), 2367–2375. https://doi.org/10.1056/NEJMra1615439.

[3]. Yazdanpanah, L., Nasiri, M., & Adarvishi, S. (2015). Literature review on the management of diabetic foot ulcer. *World Journal of Diabetes*, *6*(1), 37–53. https://doi.org/10.4239/wjd.v6.i1.37

[4]. Zhang, P., Lu, J., Jing, Y., Tang, S., Zhu, D., & Bi, Y. (2017). Global epidemiology of diabetic foot ulceration: a systematic review and meta-analysis. *Annals of Medicine*, *49*(2), 106–116. https://doi.org/10.1080/07853890.2016.1231932

[5]. Danmusa, U. M., Terhile, I., Nasir, I. A., Ahmad, A. A., & Muhammad, H. Y. (2016). Prevalence and healthcare costs associated with the management of diabetic foot ulcer in patients attending Ahmadu Bello University Teaching Hospital, Nigeria. *International Journal of Health Sciences*, *10*(2), 219–228.

[6]. Babu Natarajan, Satheesh, Gayathri Anbumani Alamelu, Saravanakumar Parameswaran, Suriyakala Perumal Chandran, Chadapully Kolumbu Ismail Sajeeth, S. M. Fazeela Mahaboob Begum, and Anandarajagopal Kalusalingam. 2025. 'Matrix Metalloproteinases (MMPs) in Diabetic Foot Ulcers: Pathophysiology and Advances in Inhibitor Development'. Comprehensive Overview of Foot and Ankle Trauma - Diagnosis, Treatment, Sequels and Rehabilitation. IntechOpen. doi:10.5772/intechopen.1010834.

[7]. Sangeeta S, Siripuram C, Konka S, Vaithilingam K, Periasamy P, Velu RK, Kandimalla R. Biomarkers of Inflammation, Oxidative Stress, and Endothelial Dysfunction in Early Detection of Diabetic Foot Ulcers. Cureus. 2025 Apr 13;17(4):e82174. doi: 10.7759/cureus.82174. PMID: 40364880; PMCID: PMC12072064.

[8]. Priyanshu Pathak, Shatrudhan Prajapati, Shikha Yadav. Combination therapy strategies for diabetic foot ulcers: synthesizing antibiotics, growth factors, and nanocarriers in modern wound management, Therapeutic Delivery. 2026; 17: 1. https://doi.org/10.1080/20415990.2026.2699574

[9]. Syafril S. Pathophysiology diabetic foot ulcer. IOP Conf Ser Earth Environ Sci [Internet]. 2018;125:012161. Available from: http://dx.doi.org/10.1088/1755-1315/125/1/012161

[10]. Oguntibeju OO. Medicinal plants and their effects on diabetic wound healing. Vet World [Internet]. 2019;12(5):653–63. Available from: http://dx.doi.org/10.14202/vetworld.2019.653-663

[11]. Singh J, Dutta T, Kim K-H, Rawat M, Samddar P, Kumar P. "Green" synthesis of metals and their oxide nanoparticles: applications for environmental remediation. J Nanobiotechnology [Internet]. 2018;16(1):84. Available from: http://dx.doi.org/10.1186/s12951-018-0408-4

[12]. I. Kapetanovic. Computer-aided drug discovery and development (caddd): In silico chemico- biological approach. Chemico-Biological Interactions, 171, 2008, 165–176.

[13]. H. Hoeltje, W. Sippl, D. Rognan and G. Folkers. Molecular modeling, basics principles and applications (John Wiley & Sons, Chichester, U.K, 2003)

[14]. U. Rester. From virtuality to reality - virtual screening in lead discovery and lead optimization: a medicinal chemistry perspective. Current Opinion in Drug Discovery and Development, 11, 2008, 559–568.

[15]. A. Jain. Virtual screening in lead discovery and optimization. Current Opinion in Drug Discovery & Development, 7, 2004, 396–403.

[16]. Le Anh Vu, Phan Thi Cam Quyen, Nguyen Thuy Huong, In silico Drug Design: Prospective for Drug Lead Discovery, International Journal of Engineering Science Invention ISSN (Online): 2319 – 6734, ISSN (Print): 2319 – 6726, Volume 4 Issue 10, 2015, PP.60-70.

[17]. C.A. Lipinski, F. Lombardo, B.W. Dominy, P.J. Feeney, Experimental and computational approaches to estimate solubility and permeability in drug discovery and development settings. Adv.Drug.Delivery Rev. 23, 4-25 (1997).

[18]. Douglas E. V. Pires, Tom L. Blundell, and David B. Ascher, pkCSM: Predicting Small-Molecule Pharmacokinetic and Toxicity Properties Using Graph-Based Signatures, ACS publications, American Chemical Society, DOI: 10.1021/acs.jmedchem.5b00104 J. Med. Chem. 2015, 58, 4066−4072.

[19]. Ravi S, Jyothi P, Shanmugam B, Subbaiah GV, Prasad SH, Sathyavelu Reddy K. A comprehensive review on traditional knowledge, phytochemistry and pharmacological properties of Acalypha indica L. Pharmacogn Rev [Internet]. 2021;15(30):134–85. Available from: http://dx.doi.org/10.5530/phrev.2021.15.16

[20]. Chekuri S, Lingfa L, Panjala S, Bindu KCS, Anupalli RR. Acalypha indica L. - an important medicinal plant: A brief review of its pharmacological properties and restorative potential. European J Med Plants [Internet]. 2020;1–10. Available from: http://dx.doi.org/10.9734/ejmp/2020/v31i1130294

[21]. Ganeshkumar M, Ponrasu T, Krithika R, Iyappan K, Gayathri VS, Suguna L. Topical application of Acalypha indica accelerates rat cutaneous wound healing by up-regulating the expression of Type I and III collagen. J Ethnopharmacol [Internet]. 2012;142(1):14–22. Available from: http://dx.doi.org/10.1016/j.jep.2012.04.005

[22]. Teklani PWNN PB. The important biological activities and phytochemistry of Acalypha indica. International Journal of Research in Pharmacy and Science. 2016;6(1):30–5

[23]. Khatoon Safina SDC. A comprehensive review of a healing herb: tridax procumbens linn. International Journal of Ayurveda and Pharma Research. 2017;5(4):79–83

[24]. Beck S, Mathison H, Todorov T, Calderon-Juarez E-A, Kopp OR. A review of medicinal uses and pharmacological activities of Tridax procumbens (L.). J Plant Stud [Internet]. 2018;7(1):19. Available from: http://dx.doi.org/10.5539/jps.v7n1p19

[25]. Yogesh P Talekar, Biswadeep Das, Tania paul, Deepali Y Talekar, Kishori G Apte, Pradeep B Parab. Evaluation of wound healing potential of aqueous and ethanolic extracts of tridax procumbens linn. In wistar rats. Asian Journal of Pharmaceutical and Clinical Research. 2012;5(4):141–5

[26]. A. Sophia,Dr Md. Faiyazuddin,Prawez Alam, Talib Hussain GC-MS characterization and evaluation of antimicrobial, anticancer and wound healing efficiency of combined ethanolic extract of Tridax procumbens and Acalypha indica **Publication:**Journal of Molecular Structure, Volume 1250, article id. 131678 February 2022

[27]. Pungle R, Nile SH, Makwana N, Singh R, Singh RP, Kharat AS. Green Synthesis of

Silver Nanoparticles Using the *Tridax procumbens* Plant Extract and Screening of Its Antimicrobial and Anticancer Activities. Oxid Med Cell Longev. 2022 Jun 25;2022:9671594. doi: 10.1155/2022/9671594. PMID: 35795854; PMCID: PMC9252769.

[28]. Kesavardhini K, Gharban HAJ, Nayak AK, Gayathri K, Lokeshwari B, Banu AS, Saranraj P. Eco-friendly green synthesis of zinc oxide nanoparticles using Acalypha indica L. leaf extract and their incorporation into topical formulations for acne and skin infection treatment. Sci Rep. 2026 May 30;16(1):26026. doi: 10.1038/s41598-026-55356-5. PMID: 42218239; PMCID: PMC13487229.

[29]. Ahmed SS, Alqahtani AM, Alqahtani T, Alamri AH, Menaa F, Mani RK, D R B, Kavitha K. Green Synthesis, Characterizations of Zinc Oxide Nanoparticles from Aqueous Leaf Extract of *Tridax procumbens* Linn. and Assessment of their Anti-Hyperglycemic Activity in Streptozoticin-Induced Diabetic Rats. Materials (Basel). 2022 Nov 18;15(22):8202. doi: 10.3390/ma15228202. PMID: 36431686; PMCID: PMC9696738.

[30]. Ashwini Jayachandran, Aswathy T.R., Achuthsankar S. Nair,Green synthesis and characterization of zinc oxide nanoparticles using Cayratia pedata leaf extract,Biochemistry and Biophysics Reports,Volume 26,2021,100995,ISSN 2405-5808,https://doi.org/10.1016/j.bbrep.2021.100995.

[31]. P. Ramesh [a], K. Saravanan [b], P. Manogar [c], J. Johnson [d], E. Vinoth [d], M. Mayakannan [d]Green synthesis and characterization of biocompatible zinc oxide nanoparticles and evaluation of its antibacterial potential Received 11 November 2020, Revised 6 January 2021, Accepted 7 January 2021, Available online 12 January 2021, Version of Record 30 January 2021.

[32]. Jaimes AK, Ayala-Peña V, Buzzi A, Álvarez V, Lassalle V. Polymeric Hydrogels Loaded with ZnO Nanoparticles as Promising Tools for Tacking Viral Skin Disorders. Viruses. 2026 Jan 5;18(1):76. doi: 10.3390/v18010076. PMID: 41600841; PMCID: PMC12846630.

[33]. Si-Yi Ma, Peng-Fei Jia, Zu-Xiu Yin, Xiao-Jie Zhang, Bo-Ya Han, Phathutshedzo Khangale, Ting-Ting Huang, Er-Peng Zhou, Juan Wang,CGG-strengthened PVA hydrogel enables pH/glucose-responsive ZnO delivery for diabetic wound healing,Materials Chemistry and Physics,Volume 3592026,132472,ISSN 0254-0584,https://doi.org/10.1016/j.matchemphys.2026.132472.

[34]. MuhammadHusnain Design and Characterization of Zinc Oxide Hydrogel Nanocomposites for Antibacterial Wound Dressing Applications October 2025Journal for Current Sign 3(4):513-538 https://www.researchgate.net/publication/397130915

[35]. Yu L, Dai Z, Huang Y, Tang S, Zhou L, Zhao X, Que X, Shi R, Zhou J, Dong J, Wang F, Gu Y. A temperature-sensitive chitosan hydrogels loaded with nano-zinc oxide and exosomes from human umbilical vein endothelial cells accelerates wound healing. Regen Ther. 2025 May 17;30:63-74. doi: 10.1016/j.reth.2025.04.020. PMID: 40491560; PMCID: PMC12146491.

[36]. Mallanagoudra, P.; M Ramakrishna, S.S.; Jaiswal, S.; Keshava Prasanna, D.; Seetharaman, R.; Palaniappan, A.; Kini, S. Progressive Hydrogel Applications in Diabetic Foot Ulcer Management: Phase-Dependent Healing Strategies. *Polymers* **2025**, *17*, 2303. https://doi.org/10.3390/polym17172303

[37]. Shrivastav A, Kumar Mishra A, Abid M, Ahmad A, Fabuzinadah M, Khan NA. Extracts of Tridax procumbens linn leaves causes wound healing in diabetic and Non-diabetic laboratory animals. Wound med [Internet]. 2020;29(100185):100185. Available from: http://dx.doi.org/10.1016/j.wndm.2020.100185

[38]. Gupta A, Upadhyay NK, Sawhney RC, Kumar R. A poly-herbal formulation accelerates normal and impaired diabetic wound healing: Wound healing efficacy of a poly-herbal formulation. Wound Repair Regen [Internet]. 2008;16(6):784–90. Available from: http://dx.doi.org/10.1111/j.1524-475X.2008.00431

[39]. Ali R, Khamis T, Enan G, El-Didamony G, Sitohy B, Abdel-Fattah G. The healing capability of clove flower extract (CFE) in streptozotocin-induced (STZ-induced) diabetic rat wounds infected with multidrug resistant bacteria. Molecules [Internet]. 2022;27(7):2270. Available from: http://dx.doi.org/10.3390/molecules27072270

[40]. Wang J, Zhang CN, Xu X, Sun TC, Kong LC, Ning RD. In Situ Formation of Hydrogels Loaded with ZnO Nanoparticles Promotes Healing of Diabetic Wounds in Rats. ACS Omega. 2024 Dec 17;9(52):51442-51452. doi: 10.1021/acsomega.4c08537. PMID: 39758615; PMCID: PMC11696414.

[41]. Di Xiao, Yingyi Huang, Zhonghan Fang, Danyang Liu, Qi Wang, Yichen Xu, Ping Li, Jiang Li,Zinc oxide nanoparticles for skin wound healing: A systematic review from the perspective of disease types,Materials Today Bio,Volume 34,2025,102221,ISSN 2590-0064,https://doi.org/10.1016/j.mtbio.2025.102221.

[42]. Muthukumar B, Nandini MS, Elumalai P, Balakrishnan M, Satheeshkumar A, AlSalhi MS, Devanesan S, Parthipan P, Rajasekar A, Malik T. Enhancement of cell migration and wound healing by nano-herb ointment formulated with biosurfactant, silver nanoparticles and *Tridax procumbens*. Front Microbiol. 2023 Aug 2;14:1225769. doi: 10.3389/fmicb.2023.1225769. PMID: 37601383; PMCID: PMC10434256.

[43]. Venkatesan U, Muniyan R. "Therapeutic potential of Acalypha indica L. leaf fractions against foodborne pathogens: an in vitro and in silico study". Sci Rep. 2025 Dec 19;16(1):2423. doi: 10.1038/s41598-025-32216-2. PMID: 41419780; PMCID: PMC12820239.

[44]. Green Synthesis and Characterization of SiO2 Nanoparticles Using Tridax Procumbens Leaf Extract and Enhancing the Invitro Wound Healing Activity in L929 Fibroblast Cell Lines Vanathi Palanimuthu1 · Nishanthi Rajendran1 · Rajiv Periakaruppan2 · Valentin Romanovski3 ·Priyanka Govindaraju1 · Mani Natarajan4 received: 11 April 2025 / Accepted: 17 October 2025 / Published online: 24 October 2025